Ju, Yuchen; Hu, Xinyi; Jokisalo, Juha; Kosonen, Risto; Xue, Tianchen; Meriläinen, Altti; Kosonen, Antti

Cost-optimal dimensioning of hybrid heat pump systems utilizing waste heat from hydrogen production for a kindergarten in cold climate

Published in:
Energy and Buildings

DOI:
10.1016/j.enbuild.2025.115430

Published: 01/04/2025

Document Version
Publisher's PDF, also known as Version of record

Energy & Buildings 332 (2025) 115430

Contents lists available at ScienceDirect

Energy & Buildings

journal homepage: www.elsevier.com/locate/enb

Cost-optimal dimensioning of hybrid heat pump systems utilizing waste heat from hydrogen production for a kindergarten in cold climate

Yuchen Ju [a,*], Xinyi Hu [b], Juha Jokisalo [a], Risto Kosonen [a,c], Tianchen Xue [a], Altti Meriläinen [d], Antti Kosonen [d]

[a] Department of Mechanical Engineering Aalto University Espoo Finland
[b] Department of Electrical Engineering and Automation Aalto University Espoo Finland
[c] College of Urban Construction Nanjing Tech University Nanjing China
[d] Lappeenranta-Lahti University of Technology LUT Lappeenranta Finland

ARTICLE INFO

Keywords:
Cost-optimization
Heat pump
Hydrogen production waste heat
District heating
Kindergarten

ABSTRACT

The growing need for environmentally-friendly energy solutions encourages the integration of various renewable energy sources in buildings. District heating (DH) systems, widely applied in northern and central European countries, are efficient in transforming and integrating renewable energy sources in large-scale energy systems. With the growth of hydrogen (H_2) production, there is great potential for utilizing H_2 production excess heat. However, the cost-optimal dimensioning of hybrid heat pump systems considering H_2 production excess heat is still in its infancy. This study examined the cost-optimal dimensioning of energy systems based on the 25-year life cycle cost (LCC). Two types of heat pumps, ground source heat pump (GSHP) and air-to-water heat pump (A2WHP) equipped with photovoltaic (PV) panels have been used in tandem with a DH system to provide heat to a kindergarten in the Nordic region. The comparison included two DH tariffs: the commercial DH prices from a DH company and the zero-emission DH price derived from waste heat generated during H_2 production. The results found that the GSHP with PV and waste heat from H_2 production has the lowest LCC. The utilization of H_2 production waste heat can decrease up to 10 % of HP dimensioning because of a lower DH price in the heating season.

1. Introduction

Energy production and consumption contribute to about 75 % of the European Union's (EU) greenhouse gas emissions [1]. It is crucial to decarbonize the energy systems to achieve the climate objectives in 2030 to cut 55 % of emissions compared with 1990 levels [1]. Buildings, as the largest single consumer, accounted for over 80 % of total EU energy production for heating, cooling, and domestic hot water (DHW) in 2023 [2]. Therefore, they need to be equipped with sustainable energy systems for carbon neutrality.

District heating systems are widely applied in northern and central European countries. For example, in Finland, district heat is the most common source of space heating. It had nearly 50 % of market share in 2020 [3]. There is a necessary transformation for the integration of renewable energy sources. Fossil fuels generated heat should be decreased to reduce greenhouse gas emissions. In this regard, the utilization of heat pumps (HP) with PV systems has arisen as a promising solution [4,5]. This combination supplies heating and cooling to buildings with more renewable energy share.

Therefore, cost-optimal dimensioning has been considered when HPs are integrated for heating. Nicoletti et al. [5] defined a procedure to carry out the combined sizing of a boiler and an air-to-water heat pump (A2WHP) with PV to minimize the net present costs over 20 years of operation. Meriläinen et al. [6] investigated the cost-optimal dimensioning of ground source heat pump (GSHP) and air-to-water heat pump (A2WHP) with PV based on the 30-year life cycle cost (LCC). The results found that a 60 % partial-power-dimensioned GSHP with PV provides the lowest LCC for a Nordic townhouse. Divkovic et al. [7] presented an optimization model based on multi-objective mixed-integer linear programming to find optimal solutions for heat generation unit dimensioning considering economic and emission objectives. The results also indicated that the growth rate in heat demand had a major influence on emissions and costs while less effects on heat pump system dimensioning.

* Corresponding author.
E-mail address: yuchen.ju@aalto.fi (Y. Ju).

https://doi.org/10.1016/j.enbuild.2025.115430
Received 8 December 2024; Received in revised form 25 January 2025; Accepted 4 February 2025
Available online 6 February 2025

In addition, researchers also developed waste heat integration strategies as renovation methods for existing DH systems [8,9]. Recently, more studies focused on low-temperature waste heat sources such as from data centers, industries, or sewage waste [8]. Low-temperature heat supply temperature can be as low as 30 °C [8]. The low-grade waste is upgraded with HPs to the required supply temperatures for DH end users [10]. Kauko et al. [11] compared the utilization of waste heat with two required DH supply temperatures (low 40 °C and medium 70 °C). Although the low-temperature DH allowed more waste heat sources integrated, the pumping cost was higher. In addition, it consumed more electricity from heat pumps to upgrade waste heat temperatures, from 30 °C to 85 °C for DHW usage. In addition, Hiltunen and Syri [12] found that the utilization of data center waste heat decreased with a 24 % CO_2 emission reduction for a DH system in Espoo, Finland. Khosravi et al. [13] reflected that the average cost of electricity generation was significantly lower when using an HP with waste heat than heat-only boilers.

Since the EU set the target of producing 20 million tons of hydrogen (H_2) in total by 2030 [14], H_2 production excess heat has great potential. Based on the EU electrolysis distribution plans, up to10% of the DH demands could be covered by electrolysis waste heat utilization [15]. Saxe and Alvfors [16] analyzed the benefits of selling excess heat from hydrogen production to a Swedish DH system. The results indicated that suitable H_2 and excess heat selling prices (eg. 60 SEK/kg and 150SEK/MWh) could make the investment profitable at an interest rate of 6 % and a system life of 20 years. Swarts et al. [17] proposed an economic model to analyze the profitable distance between low-temperature electrolyzers and district heating systems for waste-heat utilization. Results showed that the economically feasible distance between electrolyzers and DH system increased with the electrolyzer's capacity and stack temperature. Schmid and Behrendt [18] evaluated the energy autarky of residential energy system utilizing waste heat for hydrogen (H_2) production for heating. They found that low-energy houses were more technically and economically feasible to energy autarky than single-family houses and multi-family houses while resulted in high annual costs including investment, maintenance and operation. Park et al. [19] provided an optimal solution for increasing renewable energy ratio of an energy system combining GSHP and H_2 excess heat for a residential apartment complex.

However, the gap of knowledge is that there is a lack of information on the buildings' energy systems design and dimensioning combined HPs and H_2 excess heat produced district heating systems. The cost-optimal dimensioning of building energy systems based on LCC considering H_2 production excess heat and how it influences on combined HP dimensioning in hybrid heated buildings are still in its infancy. Therefore, the novelty of this study is the LCC optimization of district heated building where excess heat of H_2 production is utilized and when HPs with PV panels are integrated into the same building.

This study aims to investigate the cost-optimal dimensioning of energy systems based on the 25-year net present value (NPV) of LCC. Two types of HPs (GSHP and A2WHP) were utilized as base heating with DH back up to supply heat to a Nordic kindergarten. The objective is to combine HP and standard DH that has typical high-temperature levels for existing building stock in Finland. Following the previous research, taking operational conditions into account to minimize LCC [20,21], this study is the optimization of energy systems' design capacity based on operation conditions with different DH prices. Two DH tariffs, a commercial DH price from a DH company, and the zero-emission DH price calculated based on green H_2 production waste heat were taken into account for comparison. In addition, this paper considered the A2WHP efficiency impacts on cost-optimal dimensioning.

2. Methodology

2.1. Structure of the study

Fig. 1 shows the whole simulation process. The purpose of this study is to find the cost-optimal solution of hybrid energy systems considering waste heat from H_2 production based on 25-year LCC. The optimization function is the 25-year LCC. The variables during the optimization are design capacity values of HP, DH and PV. The design capacity change will cause the variation of LCC. Therefore, the target is to find the best combinations of HP, DH and PV design capacities when the LCC is minimum.

The building model was established as shown in the first step of Fig. 1, and heating demand was calibrated based on the measurement data. In the second step, the energy systems were modeled, and the more details were introduced in section 2.3. In the optimization step, it was realized with AutoMOO considering constraints of decision variables for energy systems. In this study, two DH tariffs were selected for comparison, a commercial DH prices from a DH company [22] and the zero-emission DH prices [23] calculated based on a DH system utilizing waste heat from H_2 production. Further information about the DH prices was introduced in section 2.3.3. Finally, the cost-optimal dimensioning solutions were analyzed in the results section.

2.2. Case study building

2.2.1. Main feature and structures

The study focuses on the cost-optimal dimensioning of energy systems for a deep renovated public kindergarten located in the cold climate area of Lappeenranta, Finland. It only has one floor with the total heated floor area of 1124 m^2 and Fig. 2 shows the floor layout.

It includes two parts, the old part and the new one. The old part was renovated, and the new part was constructed in 2022. It serves 105 children and 22 adults in total. The kindergarten is open between 6:00 and 17:00 on weekdays for occupants. There is a summer holiday from the 28th of June to the 3rd of August and a winter holiday from the 24th of December to the 4th of January per year. Table 1 presents the U-values (of external walls, roof, base floor, external doors and windows) and other parameters of the studied building.

Fig. 3 shows an example of the window with blinds between panes.

2.2.2. HVAC systems

Table 2 lists the main features of HVAC and DHW systems. The indoor air temperature setpoints for heating is 22 °C for the wet clothes changing room, activity rooms and restrooms. It is 21 °C for other room types and the setpoint for cooling is 25 °C for all the rooms [24]. The airtightness and internal gains including lighting and equipment were set according to the Finnish building code [25]. The schedules of lighting, and equipment were made following the measurement data [26].

Floor heating is installed in the kindergarten and the ventilation system is mechanical balanced ventilation with heat recovery. Fig. 4 a) shows the supply water temperatures of space heating and ventilation systems as a function of outdoor temperatures. Fig. 4 b) is the ventilation supply air temperatures changed with exhaust air temperature. There is space cooling during summer periods for the kitchen, activity rooms and restrooms. Since high-temperature DH is available for the kindergarten in Lappeenranta, it was assumed that the building was connected to a current high temperature DH network (supply temperature levels:115–70 °C) which has been widely applied in Finland.

In this type of building, the ventilation system operates intermittently. Operation hours were taken based on the actual opening of the kindergarten. There is no ventilation running during weekends and holidays, summer holiday from the 28th of June to the 3rd of August and winter holiday from the 24th of December to the 4th of January. For the constant air volume (CAV) system, it only runs for two hours before

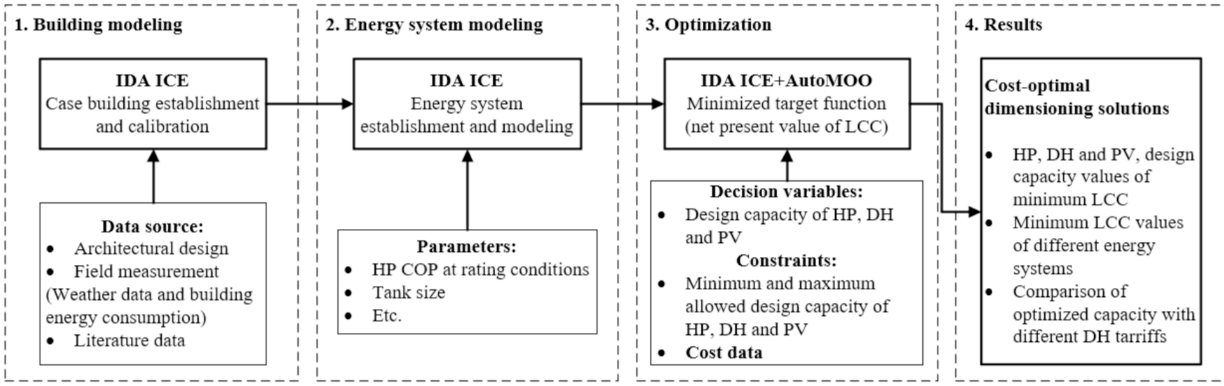

Fig. 1. The whole simulation process.

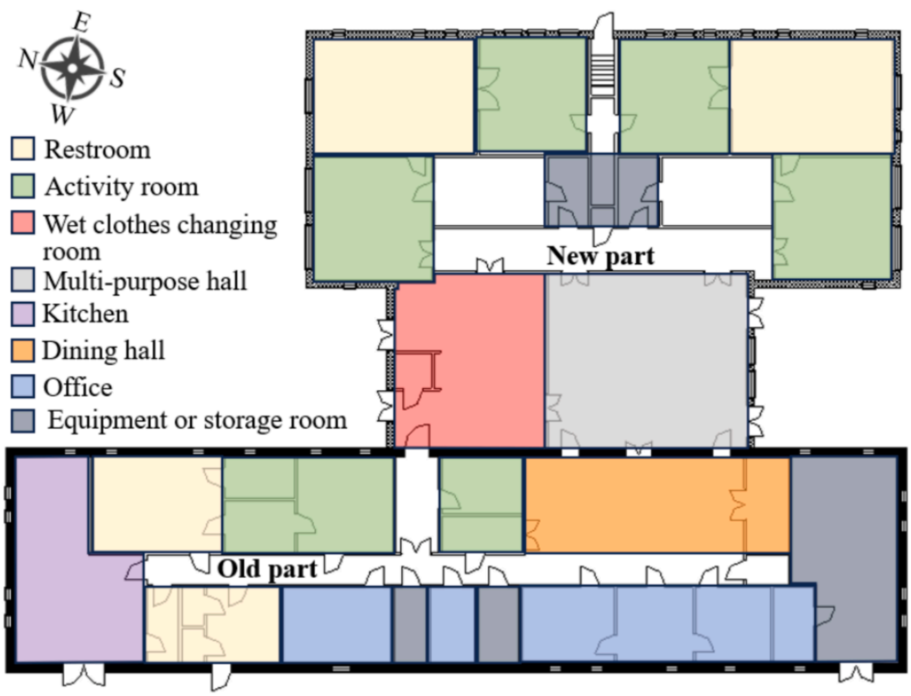

Fig. 2. The floor layout of the kindergarten.

Table 1
Building U-values and other parameters.

Parameters	Old part	New part
External walls, W/(m^{2}K)	1.0	0.17
Roof, W/(m^{2}K)	0.09	0.09
Base floor, W/(m^{2}K)	0.16	0.16
External door, W/(m^{2}K)	1.0	1.0
Windows' U-value, W/(m^{2}K)	0.9	0.9
Window shading	Blinds between panes	
Airtightness, the q_{50} value, m^3/(m^{2}h)	4	
Total heated floor area, m^2	1124	

opening at full speed to purge material emissions during workdays, which is typical in Finland based on previous studies [28,29]. After that, demand based ventilation starts to operate during occupied hours. It is CO_2-based variable air volume (VAV) system. Table 2 shows the design ranges of the ventilation airflow rates of all rooms in the building. For the VAV system, it is demand based ventilation. Air flow rates are controlled using the minimum and maximum room CO_2 level setpoints of 500 and 900 ppm. There are sensors to monitor the room CO_2 level. When the CO_2 concentration approaches or exceeds 900 ppm, air flow increases to maximum by the control damper. The air flow decreases when the CO_2 level drops below 900 ppm. The air flow varies linearly with the CO_2 level when it is between the setpoints. The air flow is at minimum, for example 0.4 L/s/m^2 when the CO_2 concentration is 500 ppm or less. However, the CAV operation mode creates significant peaks in the heating power demand during the ventilation's start-up time. The design supply and exhaust airflow rates, the pressure loss of the ventilation duct system, and the efficiencies of the fans were set based on the building design manual.

For DHW, the usage profile for weekdays shown in Fig. 5 was set based on the measurement data [26]. Percentage represents the occupants proportion of the total. There is no consumption for unoccupied hours. The DHW consumption shown in Table 2 was chosen according to the Finnish building code [25] so that the annual net DHW heating demand meets the requirement level of 11 kWh/(m^2·a) mentioned in the code for kindergarten categories.

Therefore, the dimensioning heating power (297 kW) was calculated at the design outdoor temperature (−29 °C) [25]. The dimensioning power was calculated when the heat was only supplied by DH and the internal heat gains were not taken into account.

Fig. 3. Example of window with blinds between panes.

Table 2
Main features of HVAC and DHW systems.

Parameters	Old part	New part
Heating system	Floor heating	
Dimensioning temperatures of heat distribution system, °C	35/30	
Design outdoor temperature, °C	−29	
Dimensioning heating power at design conditions, kW	297	
Ventilation system	Mechanical balanced ventilation with heat recovery	
Heat recovery efficiency	78 %	75 %
Supply and exhaust air flow rates, L/s/m^2	Restroom and activity rooms:1.5–5 Wet clothes changing room and multi-purpose hall: 1.4–4.5 Other rooms: 0.4–2.5	
Control method of space and ventilation heating systems	Supply water temperature control according to the outdoor temperature	
Cooling	Yes	
Domestic hot water consumption, m^3/m^2	0.169	
Domestic hot water supply, °C	58 [27]	

2.2.3. Weather conditions

The simulation period for LCC is the year 2023. Hourly weather data measured at the weather stations of the Finnish Meteorological Institute in Lappeenranta [30] were used in the study. They include outdoor temperature, relative humidity, wind speed and direction, and direct and diffuse solar radiation. The minimum outdoor temperature was −19.8 °C as shown in Fig. 6. The annual average outdoor temperature was 5.3 °C. The heating degree day (HDD) was calculated by adding up the differences of between the presumed indoor temperature + 17 °C and the daily average outside temperature [31]. Therefore, the total HDDs of the year 2023 was 4120 °C·d [31]. In addition, there was the building calibration based on measured heat demands from Aug. of 2022 to Aug. of 2023. The average outdoor temperature was 6.7 °C of this period with 3451 °C·d of HDDs [31].

2.2.4. Building model calibration

The building model was calibrated based on the measured DH demands from Aug. of 2022 to Aug. of 2023. Since the building was constructed and renovated in 2022, the ventilation system was used at full speed all the time for a one-year period. Therefore, the measured and simulated data were gained at this condition. The building was simulated only using the DH system. In addition, infiltration, thermal bridges, pressure coefficients and distribution system losses were adjusted in the calibration. However, during the LCC optimization simulations, the ventilation systems run as mentioned in section 2.2.2 to reflect the normal operation mode.

2.3. Energy systems

2.3.1. Properties of energy systems

Fig. 7 shows the HPs systems layout. There is a 2 m^3 buffer tank equipped to collect heat from a HP and DH as a short-term storage. The size was determined based on the previous study with the same building type [32]. The maximum capacity of the tank if it is fully mixed with tank temperature difference of 30 °C is 70 kWh. The similar principle of tank connections has been employed in previous studies [33,34]. Commercial tank has been utilized in the modelling with five inlets and five outlets in total [35].

The return water of space heating and ventilation mixes in the tank. The supply water of DH and HP go through the heat exchangers and heat up the water for space heating, ventilation and DHW. There is also the third heat exchanger for DHW. The cold city water (5 °C) connects to the heat exchanger inlet and is heated for DHW supply. The heat exchangers were dimensioned based on rating conditions to guarantee enough heat supply.

This study selected two widely applied HP types in Finland for LCC optimization. Therefore, the system combination is a ground source heat pump (GSHP) as base heating and DH as a backup with PV panels, and an outdoor air-to-water heat pump (A2WHP) with DH and PV. In Fig. 7, for the GSHP, the heat source is underground water. For the A2WHP, heat source is outdoor air. The HP connect to the tank via a heat exchanger to supply basic heat demand to the kindergarten. Similarly, DH is the backup heating. PV connects to the kindergarten electrical system and firstly supply generated electricity to the building. The surplus electricity is sold to the local market.

The heat demand is firstly covered by a HP, and the rest is supplied by DH. There is a sensor located in the tank to measure its temperature. When the storage tank supplies heat to the building, the measured temperature decreases. At every simulation time step, there is a PI controller that compares the measured temperature and the required temperature for the building side (e.g. DHW supply temperature). If the measured water temperature is lower than the required temperature, the PI controller sends a control signal firstly to the HP motorized valve to increase the mass flow for more heat supply. If HPs heat is insufficient, another signal is send to DH for extra heat.

The COP of GSHP at rating condition was set at 4.32 (0/35 °C) and the COP of A2WHP two products at rating condition (7/45 °C) was set at 3.52 based on real HP products [37].

2.3.2. Decision variables and cost data

The optimization target was formed by setting up and using the decision variables and the corresponding cost data in the dynamic energy simulations to find the cost-optimal solution (minimum LCC). The decision variables (design capacity of HP, DH and PV) change will lead to

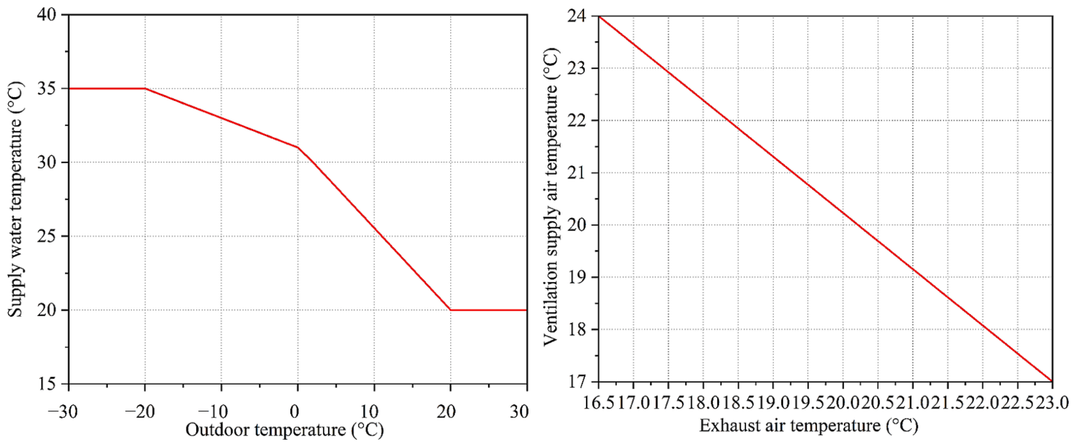

Fig. 4. Control method of space and ventilation heating systems. a). Space heating and ventilation supply water temperatures b). Ventilation supply air temperatures controlled controlled with outdoor temperatures. with exhaust air temperatures.

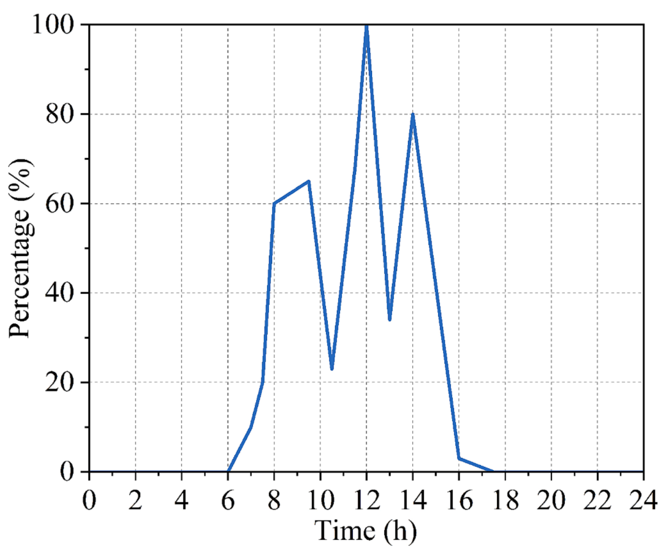

Fig. 5. DHW weekday consumption profile.

different LCC. Therefore, the objective is to find the best combinations of HP, DH and PV design capacities that minimize the LCC. The variables are all continuous. Table 3 presents the ranges of the variables' values that will change from the minimum to maximum during the optimization process for the solution of minimum LCC.

Two types of widely applied HPs (GSHP and AW2HP) in Finland were selected for cost-optimal dimensioning. Since the variation of outdoor temperatures has obvious impacts on A2WHP efficiency while the heat source of GSHP has a smaller temperature variation, two A2WHP products was examined in this study. Therefore, there are three energy systems scenarios for LCC optimization. Scenario 1 has a GSHP as base heating and DH as a backup with PV panels. The other two scenarios both have A2WHPs with DH and PV. There were two different A2WHP products selected for analysis. The minimum constraint of HP design capacity was chosen considering the actual application of HP products in this building type. The maximum constraint for HPs and DH was determined based on the dimensioning heating demand (297 kW) shown in Table 2. However, outdoor air temperatures have an obvious impact on A2WHP efficiency. With a great drop in the outdoor temperature, the HP supply heating power also decreases. Therefore, to guarantee enough heat supply, the minimum constraint of DH is higher than it in the GSHP scenario. Besides, the HP and DH maximum design capacity should also follow Eq. (1) during the optimization.

$$P_{dim.} = P_{HP} + P_{DH} \tag{1}$$

where $P_{dim.}$ is the dimensioning heating power (297 kW), kW; P_{HP} is the HP design capacity for heating at rating conditions, kW; P_{DH} is the DH design capacity, kW.

The PV panels are installed on the roofs of the building, the limited amount of installation space was set due to the roof area towards the

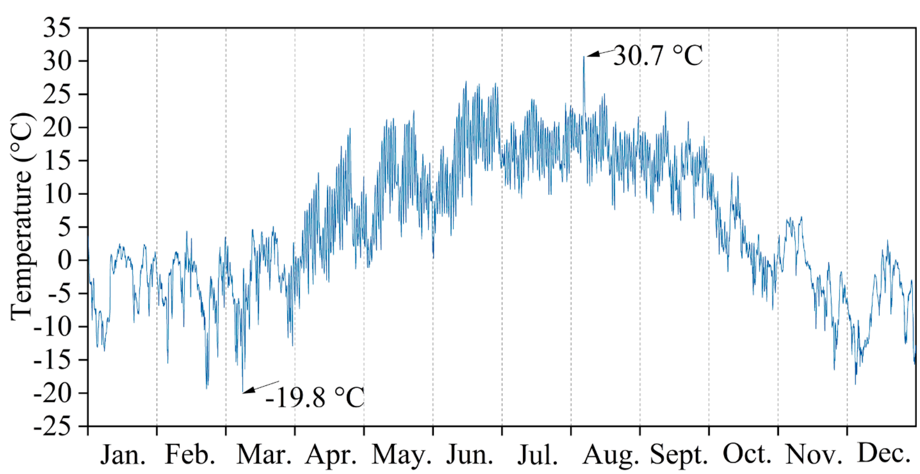

Fig. 6. The outdoor temperatures of Lappeenranta for the year 2023.

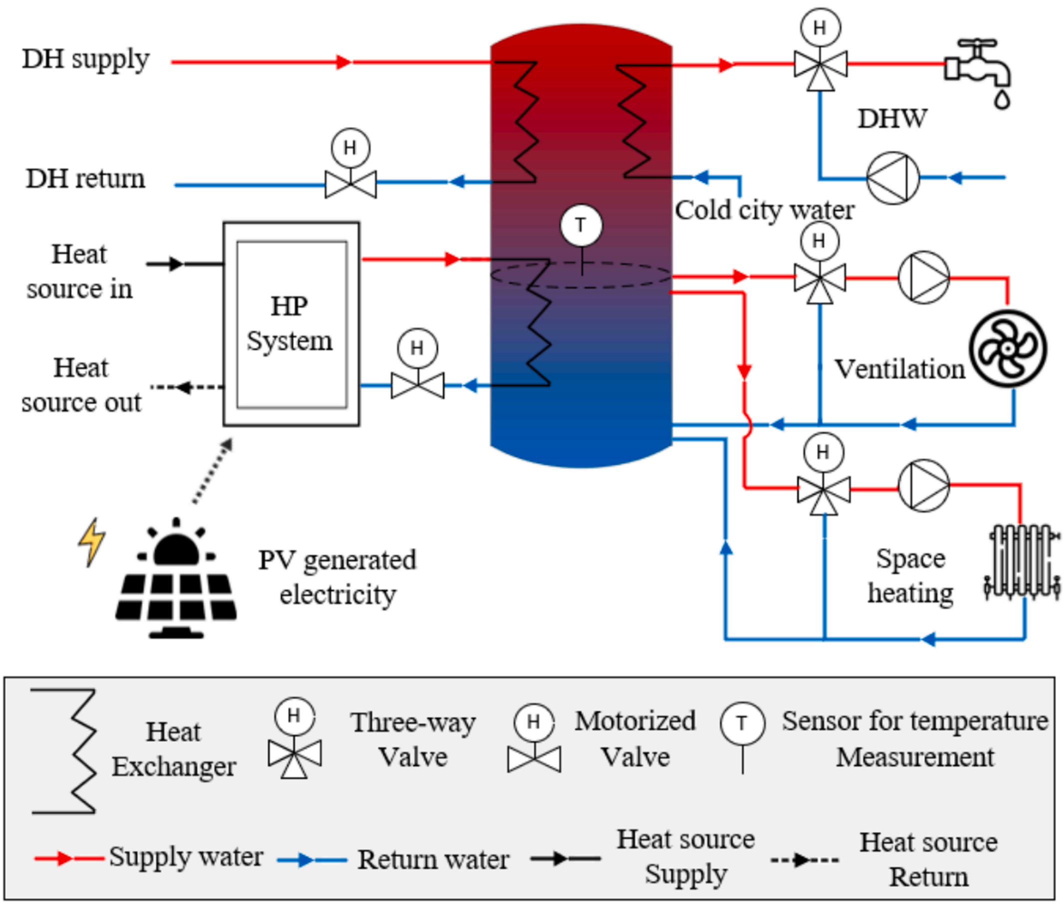

Fig. 7. HPs systems layout with PV and DH.

Table 3
Decision variables of hybrid energy systems and constraints related to them for LCC optimization.

Units	Min. value	Max. value
Scenario 1		
GSHP, kW	10	297
DH, kW	0	287
PV capacity, kW	0	61
Scenario 2		
A2WHP_1, kW	10	110
DH, kW	187	287
PV capacity, kW	0	61
Scenario 3		
A2WHP_2, kW	10	122
DH, kW	175	287
PV capacity, kW	0	61

west. Excluding the space for equipment, half of the west roof area (the maximum, 300 m^2) could be used for PV panels. Therefore, the maximum PV capacity is 61 kW.

The relevant cost data of investment (including installation), maintenance, and renewal were collected in Tables 4 and 5. Investment cost for renovating DH substation contains the costs of new substation, new heating control automation and labors. Renewal cost consists of the change fee by compressors, circulation pumps, and exchange valves along with sensors after 15 years. Since some of the original costs data gained from references were from years 2016 and 2017, the building cost index about investment cost inflation was taken into account [36]. The original ventilation system is also renewed in the renovation. The supply water temperatures for air handling units (AHU) decrease from 60 °C to 35 °C at the dimensioning condition for better HP performance.

Table 4
Investment cost data of different energy systems, all prices include a 24 % value-added tax (VAT).

System	Investment cost, including installation	Residual value after 25 years
GSHP (including borehole)	1525, €/kW [20]	50 % of the original investment cost [37]
A2WHP	780 €/kW + 18200 € [38]	50 % of the original investment cost [37]
PV	992 €/kW [6]	–
Renovation of DH substation	15,000 euro [39]	60 % of the original investment cost [37]
Tank	820 €/m^3 [32]	–
AHU coil renovation	16,000 € [40]	60 % of the original investment cost [37]

Table 5
Maintenance and renewal cost data of different energy systems (all prices include a 24 % VAT).

System	Cost
Maintenance cost of GSHP	1 % per year of the total initial investment cost [37]
Maintenance cost of A2WHP	1 % per year of the total initial investment cost [37]
Maintenance cost of PV	2 % per year of the total initial investment cost [37]
Maintenance cost of DH	0.5 % per year of the total initial investment cost [37]
Maintenance cost of AHU coil	0.5 % per year of the total initial investment cost [37]
Renewal cost for GSHP	220 €/kW after 15 years [20]
Renewal cost for A2WHP	240 €/kW after 15 years [38]

Therefore, new and bigger reheat coils were needed in the AHU to replace the old ones because of lower supply temperatures.

2.3.3. Electricity and DH prices

This study used hourly electricity prices from Nord pool, year 2023 [41]. The electricity-related costs are presented in Table 6. PV panels generated electricity was firstly served to the building. The surplus electricity was sold to the market. The hourly price of selling surplus electricity was calculated by Eq. (2):

$$p_{pv}(t) = p_{el.}(t) - F_{com.} \tag{2}$$

where $p_{PV}(t)$ is the hourly price for selling PV generated electricity, €/MWh; t is the time slot with the range from 1 to 8760, h; $p_{el.}(t)$ is the hourly electricity price from Nord pool without VAT, €/MWh; $F_{com.}$ is the commission fee (2.4 €/MWh) charged by distributors, €/MWh. There is no VAT considered for selling PV-generated electricity.

Fig. 8 shows the commercial DH prices from a DH company [22] and the zero-emission DH prices [23] used in this study. The zero-emission DH price is from the waste heat of H_2 production. It is the levelized cost of DH with VAT, which is the average production cost calculated with 6 % discount rate. It was calculated based on a waste heat recovery system including heat pumps, a pit thermal energy storage (PTES), and an electric boiler. The system DH supply temperatures were at the level 115–70 °C. The recovered waste heat from an off-grid alkaline water electrolyzer (AWE) plant was collected by PTES or heated up by HPs for heat supply to a DH network under Nordic conditions. In addition, surplus electricity (referring to solar and wind electricity) that was not utilized by the AWE plant for H_2 production was served to the HPs. More details of the system modeling and the zero-emission DH price calculation can be found in the study by Meriläinen et al. [23]. During winter time, the zero-emission DH price is much lower than the commercial DH price. The three year (2020–2022) average CO_2 emission factor of the commercial DH in Finland was 145 kg-CO_2/MWh [45] while the DH from H2 waste heat was considered as CO_2 emission free [23].

The DH cost includes DH energy costs calculated by the price shown in Fig. 8 and power fee. The power fee is charged every month. Therefore, the annual power fee was calculated by Eq. (3):

$$F_{Power}^{Annual} = F_{Power}^{Monthly} \times 12 \times P_{DHmax.} \tag{3}$$

where F_{Power}^{Annual} is the annual power fee including 24 %VAT, €; $F_{Power}^{Monthly}$ is the monthly power fee and it is 6.2 €/kW with 24 %VAT; $P_{DHmax.}$ is the annual maximum DH supply power to the kindergarten, kW.

2.4. Simulation and optimization methods

2.4.1. Simulation method

The tool IDA Indoor Climate and Energy (IDA ICE) version 5.0 was chosen for the building simulation and LCC minimization. Component models in IDA ICE are described by symbolic equations in Neutral Modeling Format (NMF) and Modelica. The equations for differential–algebraic system are solved in the general-purpose and variable time-step IDA solver. The dynamic time-step modification in simulation automatically adjusts to the problem characteristics, guaranteeing acceptable efficiency in handling transient problems [46]. Lisp programming language is applied for user interface configuration, simulation control and results access [47].

Table 6
Electricity prices with 24 % VAT and electricity tax.

Type of the fee	Price, €/MWh
Hourly electricity price from Nord pool, 2023	70.1 on average
Distribution price of electricity	47.5 [42]
Marginal value of electricity	8.1 [43]
Commission fee for selling surplus electricity, 0 %VAT	2.4 [44]

IDA ICE is one of the four main building energy simulation tools [48], addressed in studies about the validation of building simulation models. This dynamic simulation tool can model the building and systems with detailed energy consumption and indoor climate results. It dynamically calculates energy balances considering weather conditions, for example measured weather data containing air temperatures, wind direction and speed, relative humidity and etc. The heat balance equations are set based on user defined parameters about building geometry, structures, HVAC systems and internal heat gains. IDA ICE has been validated against the EN 15255–2007 and EN 15265–2007 standards [49]. In addition, several studies have provided compelling evidence for the modeling using IDA ICE in this analysis. [50–52].

The software also offers pre-configured heating and cooling systems, such as HPs, boilers and chiller. It enables components customization of the existing systems and new systems simulation. The operation of heat pump model in IDA ICE is divided into full and partial load by using specific partial load methods. The performance of heat pump at full load properties are calculated by using constant factors which are calculated from rating conditions and from the type of heat pump. The partial load properties are determined according to the full load conditions including evaporation and condensation temperatures at rated conditions, etc. In addition, the effect of temperature levels (heat source and heat distribution) on the COP and heating power output is also taken into account in the modeling. One example of a GSHP system was conducted and validated by experimental data by Graziano Salvalai [53]. Further information of HP modeling by IDA ICE can be found in Niemelä's study [54].

2.4.2. Optimization method

There are available solvers for optimization such as Gurobi or CPLEX [55]. In this study, the optimization tool used in the LCC analysis is the AutoMOO in IDA ICE. It allows automatic multi-objective optimization by running a series of simulations with systematic variation of parameters and/or changes in data structure (such as inserting or replacing different objects). A recent study indicates that AutoMOO is effective in determining cost-optimal solutions [56].

Fig. 9 presents the main optimization process by IDA ICE and AutoMOO. Firstly, decision variables and constraints are set in the tool. Secondly, the maximum generations and number of cases for each generation are set for optimization process. For example, if there are ten generations and for each there are ten cases, there will be finally a hundred optimization results.

After that, the AutoMOO starts with the first generation. The initial values of decision variables for the example ten cases are created randomly and each case will be simulated with different optimization algorithms. There are many reliable and proven optimization algorithms, including Genetic Algorithms, Evolutionary algorithms, Gradient-based algorithms [57], and others. AutoMOO will monitor and evaluate the performance of each algorithm and then select the algorithms which perform well for the specific optimization case to progress forward for the following generations. For each generation, AutoMOO compares the simulation results of objective function to decide the decision variable values for the following generation. This procedure was completed when it finalized the predetermined number of simulations.

2.4.3. Economic calculation

The cost-optimality of energy system renovation measures was determined according to the minimum NPV of the LCC using a 25-year discount period. The total NPV of the 25-year LCC was calculated by Eq. (4):

$$LCC_{NPV} = \sum I_{total} + \sum M_{total} + \sum RE_{total} - \sum RES_{total} + \sum E_{total} \tag{4}$$

where LCC_{NPV} is the NPV of the LCC for 25 years, €; $\sum I_{total}$ is the total investment cost of the energy systems and other renovation measures, €; $\sum M_{total}$ is the total maintenance cost, €; $\sum RE_{total}$ is the total renewal

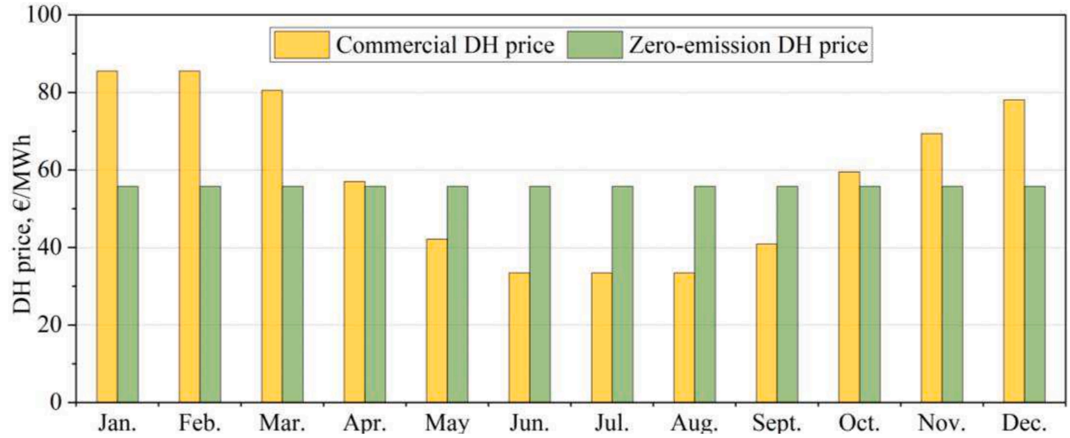

Fig. 8. DH prices with 24 % VAT.

cost, €; $\sum RES_{total}$ is the residual value of the studied measures after the 25-year discount period, €; $\sum E_{total}$ total energy cost of the studied building, €.

The total maintenance cost was calculated by Eq. (5):

$$\sum M_{total} = \frac{1-(1+r)^{-n}}{r} \times M_{annual} \tag{5}$$

where r is the real interest rate which was set as 3 % [37]; n is the discount period of the LCC calculation; M_{annual} is the annual maintenance cost, €/a.

The total energy cost was calculated by Eq. (6):

$$\sum E_{total} = \frac{1-(1+r_e)^{-n}}{r_e} \times E_{annual} \tag{6}$$

where r_e is the real interest rate for energy considered the escalation rate of energy price; E_{annual} is the annual energy cost, €/a.

The real interest rate for energy was calculated by Eq. (7):

$$r_e = \frac{i-f_e}{1+f_e} \tag{7}$$

where i is the nominal interest rate, assumed at 4 %; f_e is the escalation for energy prices, which was set at 2 % [37].

The annual energy cost was calculated by Eq. (8):

$$E_{annual} = E_{el.} + E_{DH} - E_{PV} \tag{8}$$

where $E_{el.}$ is the annual electricity cost, €/a; E_{DH} is the annual DH cost, €/a; E_{PV} is the annual income of selling surplus PV generated electricity to the market, €/a.

The total renewal cost was calculated by Eq. (9):

$$\sum RE_{total} = \frac{1}{(1+r)^k} \times RE_{annual} \tag{9}$$

where k is the year when the renewal was carried out; RE_{annual} is the renewal cost per year, €/a.

2.5. Simulated cases

Table 7 lists all the simulated cases including two reference cases that only used DH and six LCC optimization cases with HPs.

3. Results

3.1. Building model calibration results

Fig. 10 shows the monthly measured and simulated DH energy demands. The difference between measured and simulated data of each month is presented on the top of the columns. The negative values represent that simulated consumption is lower than the measured. The results are more accurate in the winter and summer periods while less accurate in the spring and fall (for example Oct. of 2022 and Apr. of 2023). A reason could be, for example, a more significant difference between the simulated and actual usage of window blinds in the spring and fall seasons than in other seasons. The difference in annual heating demand between the measured and the simulated result is −3 %.

3.2. Building hourly demand

Fig. 11 shows the kindergarten hourly heating power demand of space heating, ventilation and DHW for the year 2023. These data were utilized for LCC optimization. When the outdoor temperature dropped to the minimum, −19.8 °C, there was the maximum total heating demand, 230.5 kW.

3.3. Cost-optimal solutions

Fig. 12 shows the cost-optimal solutions of NPV of LCC changed with HP design capacity. The GSHP system provides the global optimum solution. Changing the DH price from the commercial DH prices to the zero-emission DH price decreases the minimum LCC of each case. For A2WHP cases, the cost-optimal solution is the case of product 2 with zero-emission DH prices.

Table 8 collects the results of minimum LCC and related cost-optimal dimensioning capacities of HP and DH units of the cases shown in Fig. 12. Changing the DH tariffs to the zero-emission DH price cuts the LCCs of reference cases from 583 to 542 €/m^2. For HP cases, GSHP is more beneficial (maximum 23 % of LCC reduction compared with the reference case). The system of GSHP with the renewable tariff attains the lowest capacity and LCC, indicating a more economically efficient option in comparison to the other cases. It also decreases the design capacity of both HP types when using a lower DH price (zero-emission DH price). The A2WHP (product 1) design capacity drops most from 46 kW to 15 kW meanwhile, the DH design capacity and supply heat increase. The PV capacity ranges from 10 to 14 kW.

The design capacity of both HP types in the cost optimal solutions is between 5 and 28 % of the dimensioning heating power demand, 297 kW. It reflects that most of the peak power is covered by DH as shown in Fig. 13, which is the duration curves of kindergarten total heating demand, HP supplied heat and DH supplied power for 5000 h during the heating season of the minimum LCC solutions. The building has a narrow and sharp peak caused by intermittent ventilation operation. The A2WHP (product 1) using zero-emission DH prices, provides a more limited HP power output, requiring significant DH backup, as indicated

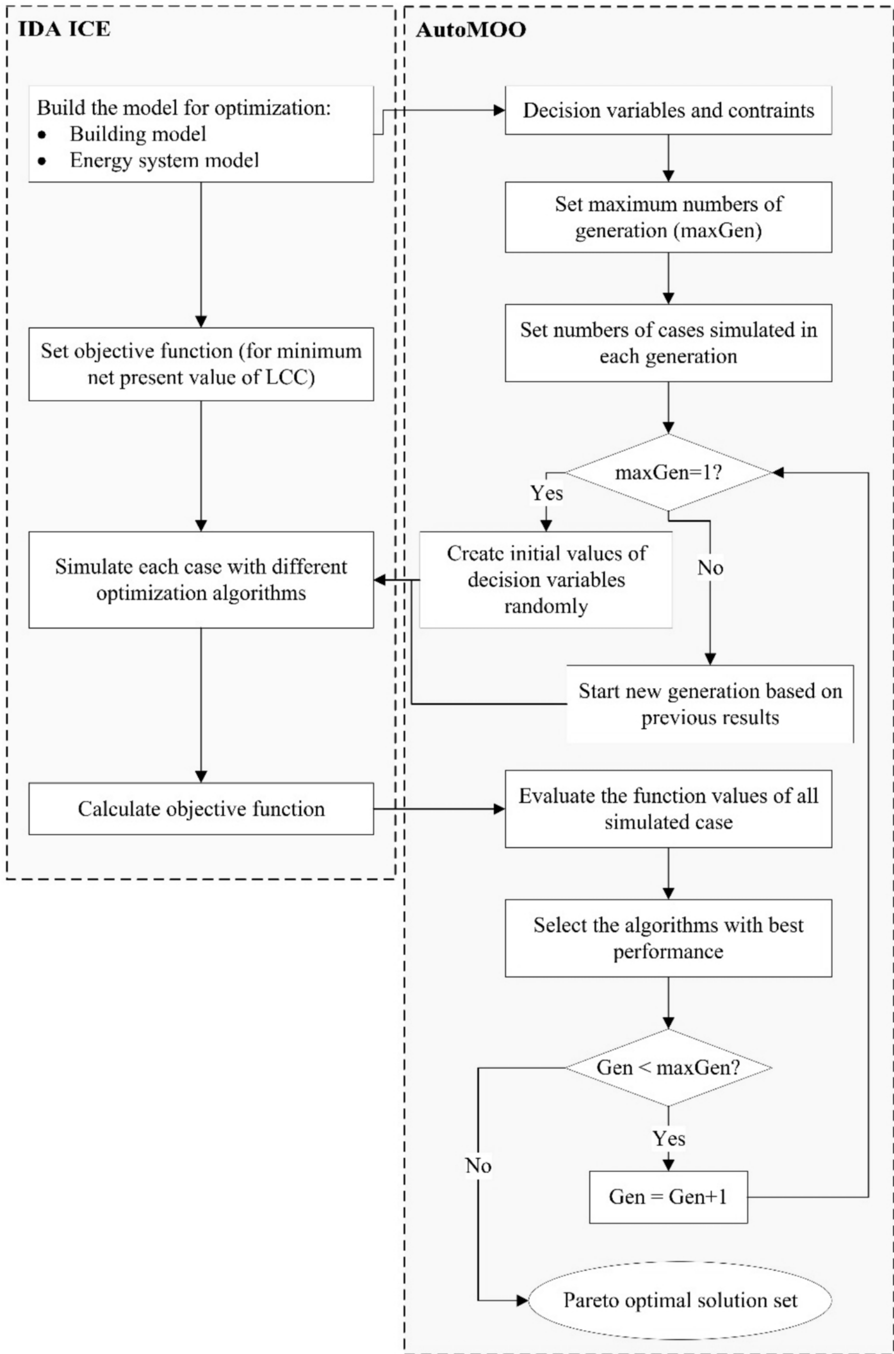

Fig. 9. Main optimization process with IDA ICE and AutoMOO for this study.

by the dashed line. The figure highlights the HP systems' heavy reliance on DH during peak periods.

However, based on the energy coverage of supply heat by HP and DH of minimum LCC solutions presented in Table 9, most of the heat demand is covered by HP. Especially, for the GSHP cases and the A2WHP (product 2), the HP as base heating accounts over 90 % of the total heat demand. Even though the A2WHP (product 1) design capacity is only 15 kW (5 % of the dimensioning heating power) with the zero-emission DH prices, it covers around 50 % of the kindergarten's heating energy demand.

Purchased energy includes building electricity and DH consumption. The purchased electricity is the building used electricity excluding the served share from PV generated. The values highlight the change of HP and DH configurations influence on the energy demand. There is a significant reduction of DH consumption after HP employed. It drops from 138 MWh for the reference case only utilized DH to the minimum around 10 MWh (GSHP and A2WHP, product 2). The system using A2WHP (product 1) with zero-emission DH prices needs the most DH because of the lowest proportion of HP supplied heat. In addition, although the PV capacity of A2WHP (product 2) is higher than that of the GSHP, the GSHP consumes less electricity than the A2WHP (product 2) to supplied over 90 % of building heating demand, owing to better HP performance during heating season.

Table 10 shows the DH costs of simulated cases when the LCC is minimum. The DH cost consists of energy cost calculated by different DH prices and power fee calculated by Eq. (3). The power fee mainly

Table 7
Simulated cases.

Reference cases	Description
Ref. DH_{com}	The building heating demand is only covered by DH with commercial DH prices.
Ref. DH_{zero}	The building heating demand is only covered by DH with zero-emission DH prices.
LCC optimization cases	
GSHP + DH_{com}	GSHP is the base heating with commercial DH prices for DH backup.
GSHP + DH_{zero}	GSHP is the base heating with zero-emission DH prices for DH backup.
A2WHP1 + DH_{com}	A2WHP product 1 is the base heating with commercial DH prices for DH backup.
A2WHP1 + DH_{zero}	A2WHP product 1 is the base heating with zero-emission DH prices for DH backup.
A2WHP2 + DH_{com}	A2WHP product 2 is the base heating with commercial DH prices for DH backup.
A2WHP2 + DH_{zero}	A2WHP product 2 is the base heating with zero-emission DH prices for DH backup.

changes by maximum DH supply power and is not affected by DH prices. Even in the reference cases when there was only DH, the proportion of power fee is still over 60 %. It is also dominant in DH cost calculation. The reason is the high peak of heating power caused by the intermittent ventilation operation of the kindergarten. The dominant role of the power fee also causes that, for the GHSP cases and the A2WHP (product 1) cases, using a lower DH price only slightly decreases the HP design capacity. Since most of the peak power is supplied by DH, for the GSHP cases and the A2WHP (product 2) cases, the share of power is over 90 %, which leads to a challenge for utilizing waste heat of H_2 production in backup heating.

3.4. A2WHP performance

HP design capacity values of A2WHP (product 2) are higher than these of the product 1 listed in Table 8. The reason is that the A2WHP (product 2) has better performance at low outdoor temperatures. Fig. 14 shows the A2WHP maximum supply power for heating of two products changed with different outdoor temperatures. The two products were tested under the same design capacity and COP. They supplied heat to the same building so the operation conditions were also the same. It can be seen that product 2 provides more heating power when the outdoor temperature is from −20 to 5 °C. With the decrease of the outdoor temperature, the difference of heating power supplied by two A2WHP products increases. Therefore, less DH was required for enough heat supply during LCC optimization periods for the product 2. It also indicates that a better HP performance during lower outdoor-temperature periods leads to higher A2WHP dimensioning capacity, lower minimum LCC, and lower total purchased energy consumption.

3.5. PV production

Table 11 collects the results of PV design capacity and generated electricity for minimum LCC solutions. The PV capacity ranges from 10 to 14 kW with the self-used PV electricity between 5.7 and 7.2 MWh. There is the highest total PV electricity generation due to the highest design capacity of A2WHP (product 2). Combining the HP design capacity values shown in Table 8, higher capacity of two HP types leads to slightly higher PV capacity. Nearly 60 % of PV-generated electricity is

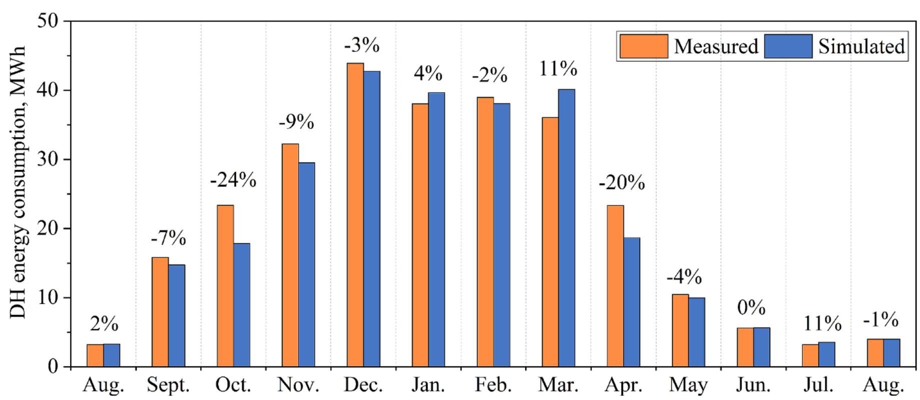

Fig. 10. Measured and simulated district heating consumption of the kindergarten from Aug. of 2022 to Aug. of 2023.

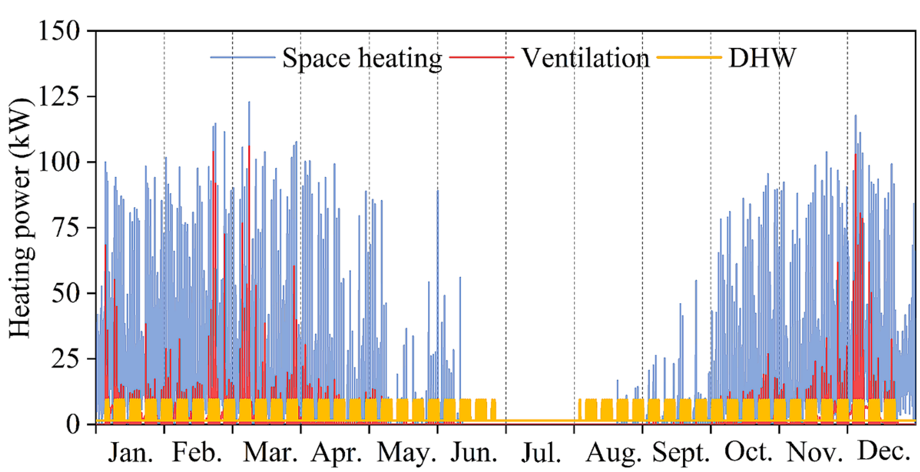

Fig. 11. Hourly heating power demand of the kindergarten for year 2023.

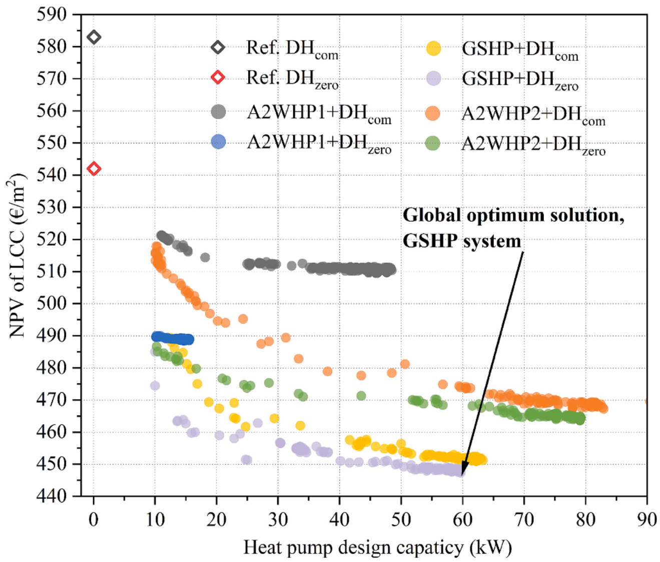

Fig. 12. Cost-optimal solutions, NPV of LCC changed with HP design capacity.

Table 8
Minimum LCC, design capacities and their shares of each case.

Cases	Minimum LCC, €/m^2	Dimensioning heating power demand, 297 kW HP design capacity, kW	DH design capacity, kW	PV design capacity, kW
Ref. DH$_{com}$	583	–	297 (100 %)	–
Ref. DH$_{zero}$	542	–	297 (100 %)	–
GSHP + DH$_{com}$	451	62 (21 %)	235 (79 %)	11
GSHP + DH$_{zero}$	447	60 (20 %)	237 (80 %)	10
A2WHP1 + DH$_{com}$	510	46 (15 %)	251 (85 %)	10
A2WHP1 + DH$_{zero}$	489	15 (5 %)	282 (95 %)	11
A2WHP2 + DH$_{com}$	467	83 (28 %)	214 (72 %)	14
A2WHP2 + DH$_{zero}$	464	79 (27 %)	218 (78 %)	13

served to the building in all cases. Both the GSHP and A2WHP cases show a relatively balanced split between self-used and sold electricity.

Fig. 15 presents the hourly purchased, exported, PV generated and total used electricity of the building with commercial DH prices for three days. The idea is to show the trading process of PV generated electricity with design capacity under difference solar density and electricity demand from the kindergarten. PV generated electricity served to the building was considered when calculating the purchased electricity. The exported electricity is the net one excluding the share supplied to the building. 10th of March was the coldest day during the heating season. Due to the lack of sunshine, PV generated electricity during daytime was fully utilized by the building without any surplus. It was normal during wintertime. For transition season, with the increase of sunshine intensity and duration, there was surplus PV generated electricity exported to the local market as shown in the middle Fig. 13th of July was the day with the maximum power of exported electricity. During the summer holiday in July, since the low requirement of electricity, PV generated electricity totally covered the building electricity during daytime and around 90 % of it was sold the local market.

Table 9
HPs and DH supplied heat and purchased energy consumption of the minimum LCC solutions.

Cases	Supplied heat, MWh HP	DH	Total	Purchased energy, MWh Electricity	DH
Ref. DH$_{com}$	–	–	134	–	138
Ref. DH$_{zero}$	–	–	134	–	138
GSHP + DH$_{com}$	123 (91 %)	12 (9 %)	135	35	12
GSHP + DH$_{zero}$	122 (91 %)	13 (9 %)	135	35	13
A2WHP1 + DH$_{com}$	108 (80 %)	27 (20 %)	135	38	28
A2WHP1 + DH$_{zero}$	63 (47 %)	71 (53 %)	135	18	73
A2WHP2 + DH$_{com}$	127 (94 %)	8 (6 %)	135	45	9
A2WHP2 + DH$_{zero}$	126 (93 %)	9 (7 %)	135	45	9

Table 10
DH costs of simulated cases when the LCC is minimum.

Cases	DH cost, €/year Energy cost	Power fee	Total
Ref. DH$_{com}$	10 647 (36 %)	18 830 (64 %)	29 477
Ref. DH$_{zero}$	8290 (31 %)	18 830 (69 %)	27 120
GSHP + DH$_{com}$	958 (7 %)	13 392 (93 %)	14 350
GSHP + DH$_{zero}$	757 (5 %)	13 541 (95 %)	14 298
A2WHP1 + DH$_{com}$	2311 (12 %)	16 428 (88 %)	18 739
A2WHP1 + DH$_{zero}$	4446 (21 %)	17 231 (79 %)	21 677
A2WHP2 + DH$_{com}$	683 (5 %)	13 295 (95 %)	13 978
A2WHP2 + DH$_{zero}$	540 (4 %)	13 459 (96 %)	13 999

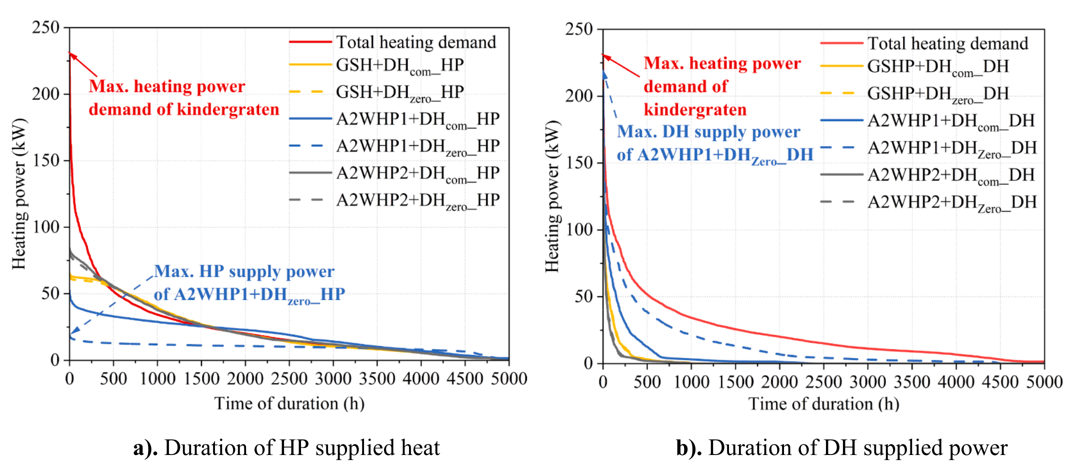

Fig. 13. Duration of kindergarten total heating demand and energy systems units supplied heating power during heating season.

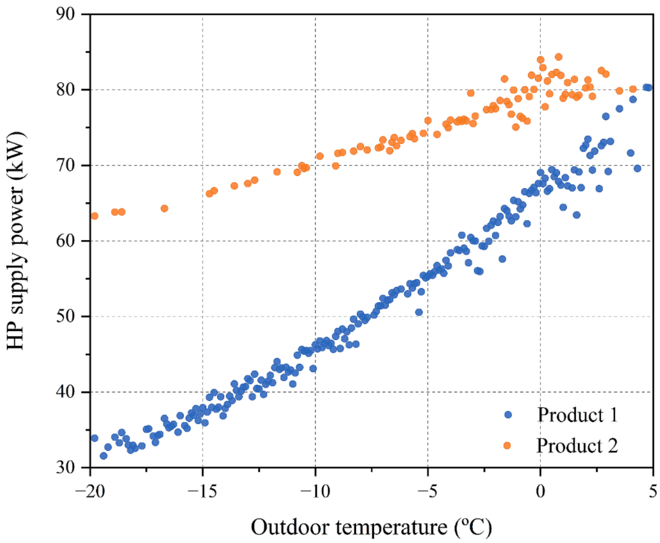

Fig. 14. The maximum A2WHP supply heating power under outdoor temperatures from −20 to + 5 °C.

Table 11
PV design capacity and generated electricity of minimum LCC solutions.

Cases	PV design capacity, kW	PV generated electricity, MWh		
		Self-used	Sold	Total
GSHP + DH_{com}	11	5.9 (58 %)	4.3 (42 %)	10.2
GSHP + DH_{zero}	10	5.7 (59 %)	4.0 (41 %)	9.7
A2WHP1 + DH_{com}	10	5.7 (59 %)	3.9 (41 %)	9.6
A2WHP1 + DH_{zero}	11	6.0 (57 %)	4.6 (43 %)	10.6
A2WHP2 + DH_{com}	14	7.2 (56 %)	5.7 (44 %)	12.9
A2WHP2 + DH_{zero}	13	7.0 (56 %)	5.4 (44 %)	12.4

4. Discussion

The cost-optimal dimensioning of building energy systems based on LCC considering H_2 production excess heat and how it influences on combined heat pump dimensioning in hybrid heated buildings were analyzed in this study. Hydrogen is anticipated to be a significant energy carrier in the transition towards renewable energy sources. Recently, some national governments have declared plans to include H_2 technologies to meet climate objectives [58]. With the increasing need for renewable H_2, the considerable energy losses associated with the water electrolysis process are indisputable. Through low-temperature electrolysis, around 60–70 % of the electrical input is converted into the product, while the remaining energy is lost as heat [15]. Therefore, DH can play a crucial role for sustainable and more efficient energy systems in the future. Low-grade renewables and waste heat can be utilized in 4th or 5th generation DH to provide customers at exegetically appropriate temperatures. The system efficiency of both the existing heat supply and the waste heat source can be improved with lower overall emissions.

The reliability of the cost-optimal solutions is mostly dependent upon the accuracy of the prices. The investment cost can fluctuate rapidly because of technology development, for example, PV panel costs. Another factor contributing to uncertainty is the future trend of the real interest rate or the escalation of energy prices. Reliable prediction of these factors is not possible, and an assumption must be made to calculate the 25-year life-cycle cost. In this study, the real interest rate and energy price escalation rate were chosen based on previous studies [20,37,38]. According to the research that has been done before, the increase in electricity price may make the PV application more profitable [32]. In addition, the escalation rate of the electricity or DH price may have a significant effect on the dimensioning of the GSHP systems (using DH as a backup) [20]. For example, if the price of district heating is rising rapidly, the HP system investment becomes relatively more cost-effective. Therefore, sensitivity analysis of different factors can be evaluated by doing further optimization.

Moreover, the power fee and DH price level will also affect HP dimensioning. The average commercial DH price used in this study is 70 €/MWh during heating season. In 2022, over 90 % of Finnish DH companies sold district heat with the average heat sales price (incl. VAT 24 %) over 70 €/MWh [59]. It reflects that the DH price in this study is relatively low. If higher DH prices from other DH companies are selected, the HP system application might be more profitable with a higher dimensioning power. If HPs become more popular, it may reduce the demand of DH and there by the use of H_2 production waste heat. Similarly, the rules of power fee charging are also variable in different DH companies [60,61]. In this study, district heat energy tariff has a minor impact on dimensioning, if power fee dominates in total DH costs. The situation might change when the power fee is lower. Another solution is to consider peak shaving, peak power limiting strategies [33,34] to cut the peak so that the power fee also decreases. Tank size could be also variable in further studies to find the optimal solution for peak cutting.

The biggest advantage of H_2 production waste heat for DH is that the source is CO_2 emission free if the H_2 is produced with clean electricity. However, the feasibility evaluation of the waste heat for application needs to consider the following three practical issues:

The first is the temperature level of the waste heat. Low-temperature electrolysis represents technologies supplied by feeding liquid water and operating at temperatures usually below 100 °C. Two well-established and commercially accessible technologies in this field are alkaline

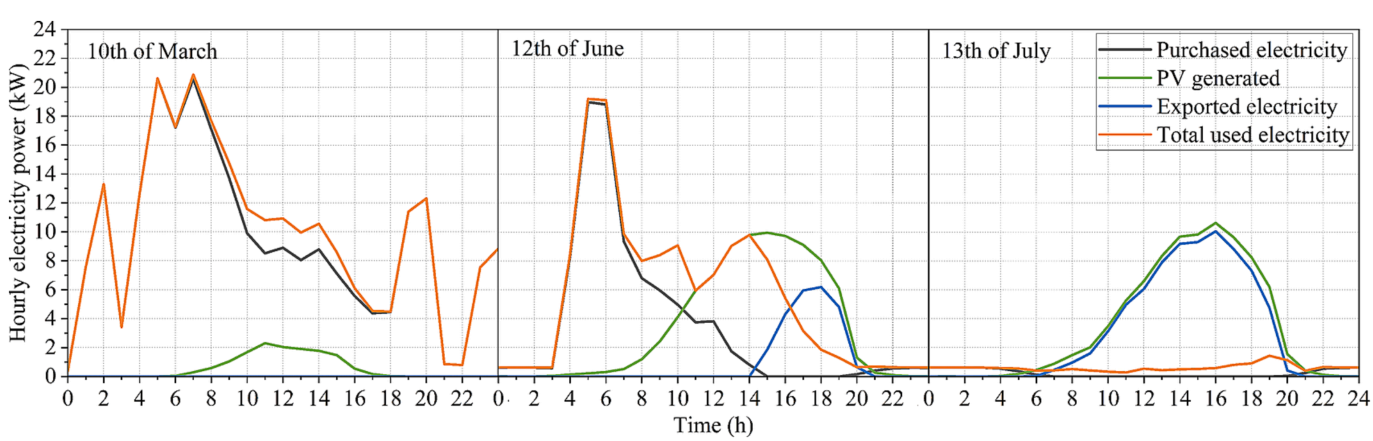

Fig. 15. Hourly values of purchased, exported, PV generated and total used electricity with commercial DH prices (GHSP + DH).

(AEL) and proton exchange membrane electrolysis (PEMEL). HPs or boilers are needed to meet the required supply temperature because of the low-temperature levels (50–80 °C for PEMEL, 60–90 °C for AEL), and additional losses of heat transfer and transportation [15].

The second issue raises about the utilization of corresponding waste heat potentials because of an increasing demand for renewable hydrogen with more installation of electrolysis plants. Electrolyzer can be more economical if the system runs more hours per year or is operated with low electricity costs [15]. A dynamic operation of low-temperature electrolysis technologies can be realized according to electricity price variation [15]. In addition, significant surpluses might arise, particularly during the summer, from waste heat by unavoidable power plant operations. Thus, heat storage is essential in the future distributed heating network for short-term or seasonal storage.

The third issue is about the distance between the H_2 production plant and the DH network. Optimization of efficiency in hydrogen production is a crucial concern for financial viability. The waste heat cannot be utilized if the electrolyzer is located far from DH networks. The type of electrolyzer generation, composition of the consumers, capacity of the local electricity network, costs of setting up a hydrogen network, and other local parameters will all affect the location of an electrolyzer. Swarts et al. [17] found that the economically feasible distance between electrolyzers and DH system increases with the electrolyzer's capacity and stack temperature.

Broadly speaking, the prospects for solar energy are promising. Considering the future, when solar PV costs decrease and storage options increase, it may be desirable to put solar panels in greater areas than now proposed for kindergartens. The architectural design of today should not impede both current and future possibilities.

The results of this study have limited direct generalizability due to the Nordic climatic conditions characterized by significant seasonal fluctuations in outdoor temperature and sun irradiation. Nevertheless, the methodology described can be applied systematically worldwide by utilizing local data on energy demand, solar PV power generation, and electricity pricing. Furthermore, the methodology applies to a wide range of buildings.

5. Conclusion

This study examined the effects of utilizing H_2 production waste heat on cost-optimal dimensioning of hybrid HP systems based on the 25-year LCC. Two types of heat pumps (GSHP and A2WHP) as base heating with DH backup have been simulated to provide heat to a kindergarten in the Nordic region. The comparison included two DH tariffs: the commercial DH prices from a DH company and the zero-emission DH price derived from waste heat generated during H_2 production. Furthermore, this work evaluated the effects of A2WHP efficiency on cost-optimal dimensioning. The results can be summarized as follows:

- The GSHP system with PV and waste heat from H_2 production has the lowest LCC among all the cases.
- Cost-optimal dimensioning of GSHP is around 20 % of the total dimensioning heating power while the dimensioning capacity of A2WHP is 5–30 % based on different HP products.
- The utilization of GSHP reduces more delivered electricity than the A2WHP.
- The results find that a better HP performance during lower outdoor-temperature periods leads to higher A2WHP capacity and lower minimum LCC.
- The zero-emission DH price is lower than the commercial DH price during heating season. Therefore, changing to use the zero-emission DH price can decrease the HP dimensioning capacity of 10 % points on optimal dimensioning.
- The energy covered by DH increases, which is beneficial for more waste heat recovered from H_2 production. However, in some cases, district heat energy tariff has a minor impact on dimensioning, if power fee dominates (accounting over 90 % of the total DH energy cost). For example, the energy coverage of GSHP is around 90 % which is a challenge for utilizing waste heat of H_2 production in backup heating.

CRediT authorship contribution statement

Yuchen Ju: Writing – original draft, Visualization, Validation, Software, Methodology, Investigation, Formal analysis, Conceptualization. **Xinyi Hu:** Writing – review & editing, Validation, Software, Methodology, Conceptualization. **Juha Jokisalo:** Writing – review & editing, Validation, Software, Resources, Methodology, Data curation, Conceptualization. **Risto Kosonen:** Writing – review & editing, Supervision, Project administration, Funding acquisition, Data curation, Conceptualization. **Tianchen Xue:** Validation, Software, Resources. **Altti Meriläinen:** Writing – review & editing, Resources, Methodology. **Antti Kosonen:** Writing – review & editing, Resources, Methodology, Funding acquisition.

Declaration of competing interest

The authors declare that they have no known competing financial interests or personal relationships that could have appeared to influence the work reported in this paper.

Acknowledgments

This study is part of the B2RECoM project funded by Business Finland and the following companies and cities participating in the project (grant number: 10784/31/2022): Aalto University Campus & Real Estate Ltd., ARCO Ltd., Elstor Ltd., Fortum Power and Heat Ltd., Gebwell Ltd., Granlund Ltd., Smart Heating Ltd., Sweco Finland Ltd., City of Helsinki, and City of Lappeenranta. The authors would like to gratefully acknowledge the partners of the B2RECoM project.

Data availability

No data was used for the research described in the article.

References

[1] Energy and the Green Deal. (2024). European Commission. Available at: https://commission.europa.eu/strategy-and-policy/priorities-2019-2024/european-green-deal/energy-and-green-deal_en (accessed on 06.08.2024).
[2] Energy Performance of Buildings Directive. (2024). European Commission. Available at: https://energy.ec.europa.eu/topics/energy-efficiency/energy-efficient-buildings/energy-performance-buildings-directive_en (accessed on 06.08.2024).
[3] Statistics on district heating. Finish Energy. (2024). https://energia.fi/en/statistics/statistics-on-district-heating/(accessed on 06.08.2024).
[4] R. Liu, Z. Liu, H. Chen, B. Li, L. Zhang, Optimal sizing and energy management strategy for an office building with photovoltaic, heat pump, thermal tank, and electric vehicle under time-of-use tariff, *Energ. Conver. Manage.* 314 (2024) 118708.
[5] F. Nicoletti, M.A. Cucumo, N. Arcuri, Cost optimal sizing of photovoltaic-battery system and air–water heat pump in the Mediterranean area, *Energ. Conver. Manage.* 270 (2022) 116274.
[6] A. Meriläinen, J.H. Montonen, A. Kosonen, T. Lindh, J. Ahola, Cost-optimal dimensioning and operation of a solar PV–BESS–heat pump-based on-grid energy system for a Nordic climate townhouse, *Energ. Buildings* 295 (2023) 113328.
[7] D. Divkovic, L. Knorr, R. Schwesig, H. Meschede, Effects on dimensioning of heat supply technologies for district heating under consideration of future developments regarding investment costs and emission factors, *Energy* 301 (2024) 131663.
[8] I. Pakere, D. Blumberga, A. Volkova, K. Lepiksaar, A. Zirne, Valorisation of Waste Heat in Existing and Future District Heating Systems, *Energies* 16 (19) (2023) 6796.
[9] M. Yuan, B.V. Mathiesen, N. Schneider, J. Xia, W. Zheng, P. Sorknæs, L. Zhang, Renewable energy and waste heat recovery in district heating systems in China: A systematic review, *Energy* (2024) 130788.
[10] S. Buffa, M. Cozzini, M. D'antoni, M. Baratieri, R. Fedrizzi, 5th generation district heating and cooling systems: A review of existing cases in Europe, *Renew. Sustain. Energy Rev.* 104 (2019) 504–522.
[11] H. Kauko, D. Rohde, A. Hafner, Local heating networks with waste heat utilization: low or medium temperature supply? *Energies* 13 (4) (2020) 954.

[12] P. Hiltunen, S. Syri, Low-temperature waste heat enabling abandoning coal in Espoo district heating system, *Energy* 231 (2021) 120916.

[13] A. Khosravi, T. Laukkanen, V. Vuorinen, S. Syri, Waste heat recovery from a data centre and 5G smart poles for low-temperature district heating network, *Energy* 218 (2021) 119468.

[14] Hydrogen. (2024). European Commission. Available at: https://energy.ec.europa.eu/topics/energy-systems-integration/hydrogen_en (accessed on 06.08.2024).

[15] H. Böhm, S. Moser, S. Puschnigg, A. Zauner, Power-to-hydrogen & district heating: Technology-based and infrastructure-oriented analysis of (future) sector coupling potentials, *Int. J. Hydrogen Energy* 46 (63) (2021) 31938–31951.

[16] M. Saxe, P. Alvfors, Advantages of integration with industry for electrolytic hydrogen production, *Energy* 32 (1) (2007) 42–50.

[17] T. Swarts, J. Morren, W. van den Akker, J.G. Slootweg, A. van Voorden, in: Techno-Economic Analysis of Low-Temperature Electrolysis' Waste-Heat Utilization, IEEE Belgrade PowerTech, 2023 June, pp. 01–06.

[18] F. Schmid, F. Behrendt, Genetic sizing optimization of residential multi-carrier energy systems: The aim of energy autarky and its cost, *Energy* 262 (2023) 125421.

[19] S.H. Park, Y.S. Jang, E.J. Kim, Multi-objective optimization for sizing multi-source renewable energy systems in the community center of a residential apartment complex, *Energ. Conver. Manage.* 244 (2021) 114446.

[20] T. Niemelä, R. Kosonen, J. Jokisalo, Cost-optimal energy performance renovation measures of educational buildings in cold climate, *Appl. Energy* 183 (2016) 1005–1020.

[21] H. ur Rehman, J. Hirvonen, R. Kosonen, K. Sirén, Computational comparison of a novel decentralized photovoltaic district heating system against three optimized solar district systems, *Energ. Conver. Manage.* 191 (2019) 39–54.

[22] Kauko-lämmön hinnat taloyh-tiöille ja yrityk-sille (District heating prices for building societies and companies). (2024). Fortum. Available at: https://www.fortum.fi/yrityksille-ja-yhteisoille/lammitys-ja-jaahdytys/kaukolampo/kaukolammon-hinnat (in Finnish, accessed on 25.07.2024).

[23] A. Meriläinen, A. Kosonen, J. Jokisalo, R. Kosonen, P. Kauranen, J. Ahola, Techno-economic evaluation of waste heat recovery from an off-grid alkaline water electrolyzer plant and its application in a district heating network in Finland, *Energy* 306 (2024) 132181.

[24] Ministry of Environment. Ympäristöministeriön asetus uuden rakennuksen sisäilmastosta ja ilmanvaihdosta Decree 1009/2017 Ministry of Environment's decree on the Indoor Climate and Ventilation of New Buildings]. Ministry of Environment. Helsinki. Finland. Available online: https://www.finlex.fi/fi/laki/alkup/2017/20171009.

[25] Ministry of Environment. Ympäristöministeriön asetus uuden rakennuksen energiatehokkuudesta [Decree 1010/2017 Ministry of Environment's decree on the Energy Performance of New Buildings]. Ministry of Environment. Helsinki. Finland. Available online: https://www.finlex.fi/fi/laki/alkup/2017/20171010.

[26] J. Nyman, *Cost Optimal Heating and Cooling Systems in Nearly Zero Energy Service Buildings (master's Thesis)* (2016) accessed on January 12, 2025, https://aaltodoc.aalto.fi/items/4211e4e0-424e-4766-ba3f-450a56ff297d.

[27] Publication K1/2021. Rakennusten kaukolämmitys-Määräykset ja Ohjeet-Julkaisu K1/2021(District Heating of Buildings-Regulations and Guidelines-Publication K1/2021). Energiateollisuus. Available online: https://lnkd.in/gsyNvwk2 (accessed on 12 August 2022). (In Finnish).

[28] Lestinen S, Kilpeläinen S, Kosonen R and Jokisalo J. (2021). Effects of ventilation use in non-occupied conditions on indoor air quality. ROOMVENT 2020: Energy Efficient Ventilation for Healthy Future Buildings. 15-17.2 2021 Turin (virtual conference).

[29] S. Lestinen, S. Kilpeläinen, R. Kosonen, Julkisten rakennusten ilmanvaihdon käyttöaikojen vaikutus työolosuhteisiin ja sisäilman laatuun-Työsuojelurahaston hanke 180094 (The effect of ventilation operating hours in public buildings on working conditions and indoor air quality-Työsuojelurahastos project), Aalto University Publication series Science, 2021. + technology 3/2021. ISBN 978-952-64-0413-4 (in Finnish).

[30] Finnish Meteorological Institute. (2023). Weather and Sea—Download Observations. Available at: https://en.ilmatieteenlaitos.fi/download-observations (accessed on 30.08 2024).

[31] Finnish Meteorological Institute. (2023). Heating degree days Available online: https://en.ilmatieteenlaitos.fi/heating-degree-days?7r87D3pXt5h3S3AkDpM0uF_q=y%253D2023 (accessed on 02 October 2023).

[32] P. Sankelo, J. Jokisalo, J. Nyman, J. Vinha, K. Sirén, Cost-optimal energy performance measures in a new daycare building in cold climate, *Int. J. Sustain. Energ.* 38 (2) (2019) 104–122.

[33] Y. Ju, J. Jokisalo, R. Kosonen, Peak shaving of a district heated office building with short-term thermal energy storage in Finland, *Buildings* 13 (2023) 573.

[34] Y. Ju, P. Hiltunen, J. Jokisalo, R. Kosonen, S. Syri, Benefits through Space Heating and Thermal Storage with Demand Response Control for a District-Heated Office Building, *Buildings* 13 (10) (2023) 2670.

[35] High quality Akvaterm accumulators, tanks and hot water heaters - also custom-made according to measures. Made in Finland. (2025). AKVATERM. Available at: https://akvaterm.fi/en/(accessed on 23.01.2025).

[36] Building cost index. (2024). Statistic Finland. Available at: https://stat.fi/en/statistics/rki (accessed on 25.07.2024).

[37] T. Niemelä, R. Kosonen, J. Jokisalo, Cost-effectiveness of energy performance renovation measures in Finnish brick apartment buildings, *Energ. Buildings* 137 (2017) 60–75.

[38] T. Niemelä, R. Kosonen, J. Jokisalo, Energy performance and environmental impact analysis of cost-optimal renovation solutions of large panel apartment buildings in Finland, *Sustain. Cities Soc.* 32 (2017) 9–30.

[39] HögforsGST. (2024). Substations. Available at: https://hogforsgst.com/en/products/substations/(accessed on 10 Mar. 2024).

[40] T. Xue, J. Jokisalo, R. Kosonen, Y. Ju, Design of High-Performing Hybrid Ground Source Heat Pump (GSHP) System in an Educational Building, *Buildings* 13 (7) (2023) 1825.

[41] Day-ahead prices. (2024). Nord pool. Available at: https://data.nordpoolgroup.com/auction/day-ahead/prices?deliveryDate=2024-02-16&currency=EUR&aggregation=Hourly&deliveryAreas=AT,FI (accessed on 25.07.2024).

[42] Price of electricity by type of consumer, 2008M01-2024M03. (2024). Statistic Finland. Available at: https://pxdata.stat.fi/PxWeb/pxweb/en/StatFin/StatFin_ehi/statfin_ehi_pxt_13rb.px/(accessed on 25.07.2024).

[43] Sähkösopimus yritykselle (Electricity contract for the company). (2024). Fortum. Available at: https://www.fortum.fi/yrityksille-ja-yhteisoille/sahkosopimus-yritykselle/sahkosopimukset?products=10&usage=100000 (in Finnish, accessed on 25.07.2024).

[44] Myy ylimää-räinen uusiutuva sähkösi meille (Sell your excess renewable electricity to us). (2024). Fortum. Available at: https://www.fortum.fi/kotiasiakkaille/sahkoa-kotiin/uusiutuva-energia/oman-tuotannon-myynti-lahisahko?vtab=accordion-item-108823 (in Finnish, accessed on 25.07.2024).

[45] CO2-päästökertoimet (CO2 emission factors). (2024). Motiva. Available at: https://www.motiva.fi/ratkaisut/energiankaytto_suomessa/co2-paastokertoimet (in Finnish, accessed on 24.11.2024).

[46] Per Sahlin, Modelling and Simulation Methods for Modular Continuous Systems in Building, Royal Institute of Technology (1996).

[47] C. Fu. (2020). Automation of Building Energy Performance Simulation with IDA ICE, KTH Royal Institute of Technology. Master's thesis. Available at https://urn.kb.se/resolve?urn=urn:nbn:se:kth:diva-284528 (accessed on January 09, 2025).

[48] K. Hilliaho, J. Lahdensivu, J. Vinha, Glazed space thermal simulation with IDA-ICE 4.61 software—Suitability analysis with case study, *Energ. Buildings* 89 (2015) 132–141.

[49] Equa Simulation, A.B. *Validation of IDA Indoor Climate and Energy 4.0 with Respect to CEN Standards EN 15255-2007 and EN 15265-2007*; EQUA Simulation Technology Group: 2010. Available online: http://www.equaonline.com/iceuser/CEN_VALIDATION_EN_15255_AND_15265.pdf (accessed on 11 February 2023).

[50] A. Bring, P. Sahlin, M. Vuolle, *Models for Building Indoor Climate and Energy Simulation–A report of IEA SHC Task 22: Building Energy Analysis Tools*, Stockholm, Sweden IEA, 1999.

[51] Equa Simulation, A.B. *Validation of IDA Indoor Climate and Energy 4.0 build 4 with Respect to ANSI/ASHRAE Standard 140-2004*; EQAU Simulation Technology Group: 2010. Available online: http://www.equaonline.com/iceuser/validation/ASHRAE140-2004.pdf (accessed on 11 February 2023).

[52] Moosberger, S. IDA ICE CIBSE-Validation: Test of IDA Indoor Climate and Energy version 4.0 according to CIBSE TM33, issue 3. *HTA LUZRN/ZIG*: 2007. Available online: http://www.equaonline.com/iceuser/validation/ICE-Validation-CIBSE_TM33.pdf (accessed on 11 February 2023).

[53] EQUA Simulation AB, "Exhaust air heat pump for residential," Available online: https://www.equa.se/en/ida-ice/case-studies/exhaust-air (accessed on January 12, 2025).

[54] Niemelä, T. (2018). Cost-optimal renovation of residential, educational and office buildings in Finnish climate toward nearly zero-energy buildings. Doctoral thesis. Available at: https://urn.fi/URN:ISBN:978-952-60-7814-4 (accessed on January 12, 2025).

[55] M. Sameti, F. Haghighat, Optimization approaches in district heating and cooling thermal network, *Energ. Buildings* 140 (2017) 121–130.

[56] X. Hu, J. Jokisalo, R. Kosonen, M. Lehtonen, T. Shao, Cost-optimal renovation solutions for detached rural houses in severe cold regions of China, *Buildings* 13 (3) (2023) 771.

[57] V. Machairas, A. Tsangrassoulis, K. Axarli, Algorithms for optimization of building design: A review, *Renew. Sustain. Energy Rev.* 31 (2014) 101–112.

[58] Key actions of the EU Hydrogen Strategy (2024). European Commission. Available at: https://energy.ec.europa.eu/topics/energy-systems-integration/hydrogen/key-actions-eu-hydrogen-strategy_en (accessed on 09.10.2024).

[59] District heating statistics. (2024). Finnish Energy. Available at: https://energia.fi/en/statistics/district-heating-statistics/(in Finnish, accessed on 09.09.2024).

[60] Hinnat – Kuukausilämpö Koti (Prices – Monthly heat home). (2024). Helen. Available at: https://www.helen.fi/lammitys/kaukolampo/hinnat (in Finnish, accessed on 09.09.2024).

[61] Hinnasto (Price list). (2024). Alajärven Lämpö Oy. Available at: https://www.alajarvenlampo.fi/49-2/(in Finnish, accessed on 09.09.2024).